Original article

Nuclear Medicine Communications

Metabolic imaging patterns in posterior cortical atrophy and Lewy body dementia

Vanshika Gupta[a], Ritu Verma[a], Rajeev Ranjan[b], Ethel S. Belho[a], Nikhil Seniaray[a], Veronique Dinand[c], Dharmender Malik[a] and Harsh Mahajan[d]

Purpose: **To study the imaging patterns of Posterior cortical atrophy (PCA) and Dementia with Lewy bodies (DLB) on fluoro-deoxyglucose positron emission tomography computed tomography ([^{18}F]FDG PET/CT), identify areas of overlap and differences and to develop a prediction model to assist in diagnosis using univariate and multivariate analysis.**

Methods: **A retrospective analysis of 72 patients clinically suspected of having posterior dementia was done. All patients underwent [^{18}FF]FDG PET/CT of the brain and dopamine transporter imaging with [[^{99m}Tc] TRODAT-1 SPECT scan on separate days. The patients were divided into PCA with normal TRODAT uptake (n=34) and DLB with abnormal TRODAT uptake (n=38). The FDG PET/CT uptake patterns were recorded and areas of significant hypometabolism by z score analysis were considered as abnormal. Receiver operator characteristics (ROC) curve analysis was used to determine cutoff z scores and binary logistic regression analysis was used to determine the Odds ratio of being in the predicted groups.**

Results: **Significantly hypometabolism was found in parieto-temporo-occipital association cortices and cingulate cortices in PCA patients. DLB patients showed significantly reduced uptake in the visual cortex. No significant difference was found between z score of occipital association cortex which showed hypometabolism in both groups. The cut-off z-score values derived from the ROC curve analysis were as follows- parietal association (cut-off-3, sensitivity-65.6%, specificity - 68.7%), temporal association (cut-off-2, sensitivity-78%, specificity-75%) and posterior cingulate (cut-off-0.5, sensitivity-93.7%, specificity-40.6%), their respective Odds ratio (with 95% confidence interval) for being in the PCA group as derived from univariate logistic regression were 3.66 (1.30–10.32), 10.71 (3.36–34.13) and 7.85 (1.57–39.17). The cut-off z score of primary visual cortex as derived from ROC curve was zero with sensitivity of 87.5%, specificity of 71.9%, and the Odds ratio for being the in the DLB group was 24.7 with 95% confidence interval of 5.99–101.85.**

Conclusion: **[^{18}F]FDG PET may be useful as a non-invasive diagnostic modality in differentiating the two posterior cortical dementias, despite significant overlap. Primary visual cortical hypometabolism can serve as an independent diagnostic marker for DLB, even in the absence of TRODAT imaging.** ***Nucl Med Commun*** **XXX:000–000**

Nuclear Medicine Communications 2019, **XXX**:000–000

Keywords: FDG, Lewy body dementia, PET, PET/CT, posterior cortical atrophy, TRODAT SPECT

[a]Department of Nuclear Medicine and PET-CT, Mahajan Imaging Center, Sir Ganga Ram Hospital, Departments of [b]Neurology, [c]Research, Sir Ganga Ram Hospital and [d]Mahajan Imaging Center, New Delhi, India

Correspondence to Vanshika Gupta, DNB Nuclear Medicine, Department of Nuclear Medicine and PET-CT, Mahajan Imaging Centre, Sir Ganga Ram Hospital, Rajinder Nagar, Delhi 110060, India
Tel: +9599651685, +011 42251844, +011 42251845;
fax: +91 11 42251844; e-mail: vanshikagupta.jnmc@gmail.com

Received 21 August 2019 **Accepted** 16 September 2019

Introduction

Posterior cortical atrophy (PCA), a variant of Alzheimer's disease (AD), also known as Benson's syndrome, is characterized by progressive dementia associated with progressive decline in visuospatial and visuoperceptual functions, such as simultagnosia, optic ataxia, dysgraphia and oculomotor apraxia [1,2].

Dementia with Lewy bodies (DLB) is the second most common neurodegenerative dementia following AD and is pathologically characterized by the presence of Lewy bodies in cortical, subcortical and brainstem structures. The core diagnostic features of DLB are a triad of fluctuating cognitive impairment, well-formed visual hallucinations and Parkinsonism. Rapid eye movement sleep behaviour disorder (RBD) is also considered a core manifestation of DLB [3]. Since Parkinsonism is a classical manifestation of DLB, but is preceded by dementia by at least 1 year, dopamine transporter (DAT) imaging with [^{99m}Tc]TRODAT-1 SPECT has proven useful in its diagnosis. DAT imaging has been established to assist in distinguishing DLB from AD by demonstrating decline in the density of striatal dopaminergic receptor and transporters in the former [4]. This has been utilized in our study to classify patients with clinically overlapping symptoms of posterior dementia into possible PCA (normal striatal TRODAT uptake) and probable DLB (reduced striatal TRODAT uptake) groups.

0143-3636 Copyright © 2019 Wolters Kluwer Health, Inc. All rights reserved. DOI: 10.1097/MNM.0000000000001102

Both PCA and DLB have been associated with occipital hypometabolism on [^{18}F]FDG PET scan. The presence of occipital hypometabolism has been shown to be a useful feature to differentiate both DLB [5–8] and PCA [9–11] from typical AD. Most pathological studies on PCA patients have shown that the most affected areas in this group tend to be parieto-occipital regions, over temporo-parietal as in AD.

Studies in DLB have shown that the posterior cingulate (PC) is relatively spared in these patients. This has additionally been utilized to accurately differentiate DLB from AD patients [12–14]. However, differentiating the two posterior dementias (DLB and PCA) on [^{18}F]FDG PET alone has been challenging, as it remains unclear if cingulate island sign is seen in PCA as well. This poses a contemplative diagnostic dilemma, probing research into the role of molecular and imaging biomarkers specific to the disease pathology.

We aimed to study the imaging patterns of PCA and DLB on [^{18}F]FDG PET/CT, and identify areas of overlap and differences between them. We tried to develop a prediction model to assist in the diagnosis of PCA and DLB using univariate and multivariate analysis on the core areas of hypometabolism seen on [^{18}F]FDG PET.

Methods

All procedures performed in studies involving human participants were in accordance with the ethical standards of the institutional research committee. Informed consent was obtained from all individual participants included in the study.

Patient selection

The study population consisted of cases referred to the Department of Nuclear Medicine and PET/CT. We retrospectively analyzed records of patients who underwent clinical assessment and neurological examination by a neurophysician in our hospital, and had undergone DAT imaging with [^{99m}Tc]TRODAT-1 SPECT and metabolic imaging by [^{18}F]FDG PET/CT scan in our department. Both these studies were carried out on separate days, usually consecutive working days. Only those patients who fulfilled the clinical criteria for PCA [2,15] and probable DLB [3] were recruited for the study. Inclusion criteria for PCA were insidious onset with gradual progression; visual complaints in the absence of significant primary ocular disease which could explain the symptoms; relative preservation of anterograde memory with preserved insight; disabling visual impairment throughout the disorder; and presence of any of the following simultanagnosia with or without optic ataxia or oculomotor apraxia, constructional dyspraxia, visual field defect, environmental disorientation, or any elements of Gerstmann syndrome (acalculia, agraphia, left-right disorientation and finger agnosia) [16].

Clinical DLB features that were recorded in each subject included fluctuations in cognitive impairment, motor manifestations of Parkinsonism, visual hallucinations and RBD [17].

Using TRODAT SPECT as the scintigraphic gold standard for DLB, these patients were divided into PCA (n = 34) and DLB (n = 38) groups. Patients with abnormal TRODAT scan and clinical diagnostic features meeting the said criteria were classified into probable DLB group, and those with normal TRODAT scan and visuospatial deficits as mentioned in the inclusion criteria were classified into the PCA group (Fig. 1).

Image acquisition and analysis

^{99m}Tc-labelled tropane derivative (TRODAT-1) was prepared from a preformulated lyophilized cold kit. After the intravenous injection of 20–22 mCi, brain SPECT images were acquired using a low-energy, high-resolution collimator on a GE Discovery NM 630 dual-head camera (GE Healthcare, Chicago, USA) at 4 hours post-injection. Iterative reconstruction (ordered subset expectation maximization) was done, and images were reconstructed using back-projection with a Metz filter.

All patients underwent [^{18}F]FDG PET/CT performed using a PET/CT scanner (GE Healthcare) operating in three-dimensional mode. These patients were prepared with strict 4 hours fasting before intravenous injection of ~0.15 mCi/kg of [^{18}F]FDG, provided their blood sugar levels were less than 150 mg/dl at the time of injection. Patients were made to rest in an isolated, quiet, dimly lit room for the next 45–60 minutes with their eyes open. Images were interpreted at Advantage window workstation (version 4.5; GE Healthcare) equipped with fusion software that enables the display of PET images with and without attenuation correction, CT images, and fused PET/CT images. A commercially available software application (Cortex ID; GE Healthcare) was used to obtain 3D Stereotactic Surface Projection images with z score values in core brain regions as shown in Fig. 2. The voxel-level analysis was performed using statistical parametric mapping 12 [18] after normalization using an in-built template. Group statistical comparisons were performed comparing PCA and DLB with each other using 2-sided t-tests. A conjunction analysis using the contrasts comparing each disease group with a set of standardized normative data was performed to assess regions of hypometabolism that overlapped between PCA and DLB. Left and right hemisphere values were averaged for our group comparisons because there was no evidence of statistically significant hemispheric differences at intra- and inter-group levels.

Statistical analysis

Statistical analysis was done using SPSS program for Windows, version17.0 and by the assessment of the

Fig. 1

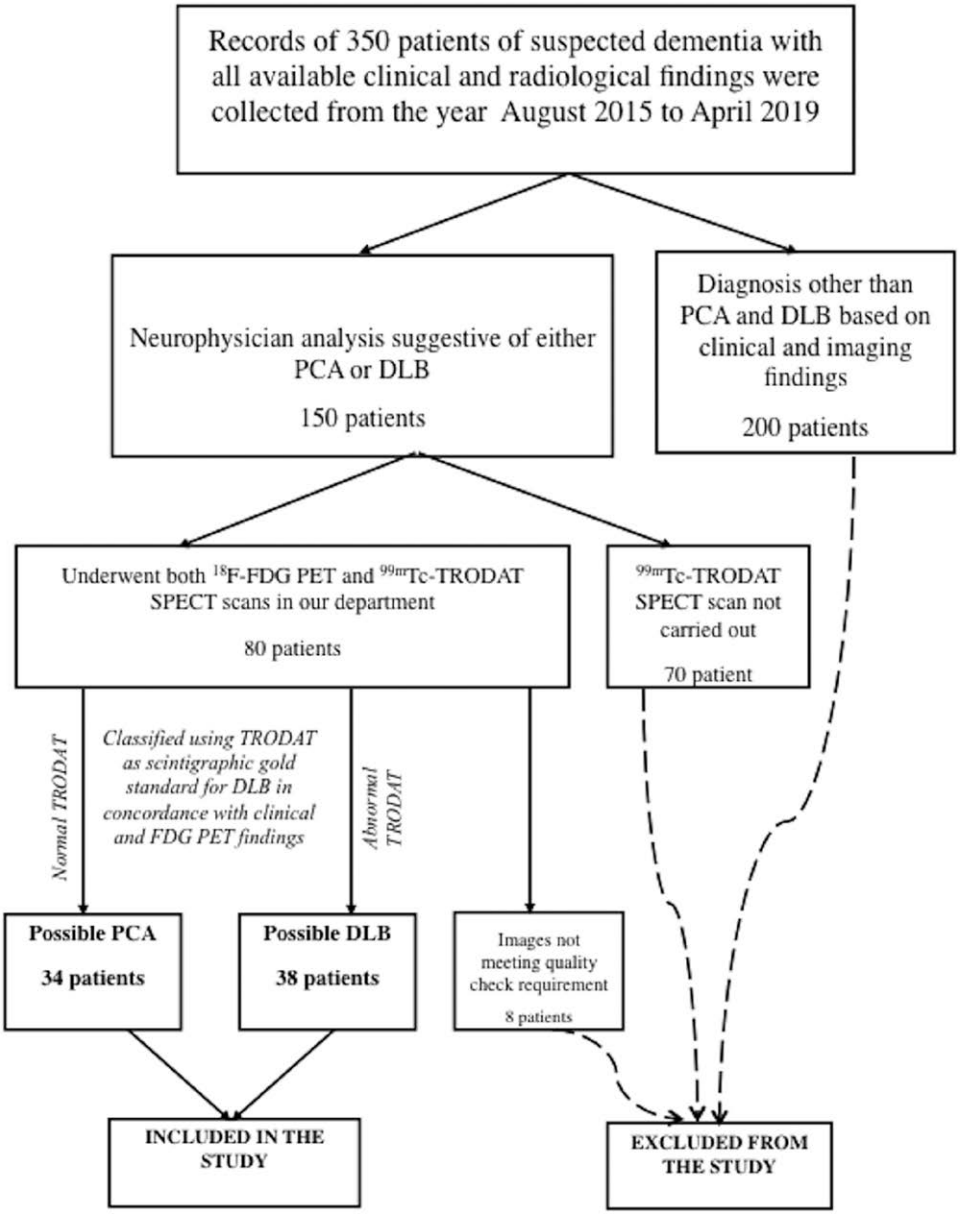

Definition of the final study group.

Z score surface maps obtained from Cortex ID (GE Healthcare, USA). The FDG uptake patterns were recorded and areas of hypometabolism in the cerebral cortex that were two SDs from the mean were considered as abnormal. Data were checked for normalcy using Shapiro-Wilk test and *t*-test was applied to determine the significance of difference between hypometabolism in both patient groups. Receiver operator characteristic (ROC) curve analysis was carried out to determine the significant cut-off values of z scores for each region with their respective sensitivity and specificity. Univariate and multivariate binary logistic regression analysis was applied to these cut-off z-scores for each region to determine the odds ratio of being in either of the two predicted groups. For all statistical tests, *P*-value of less than 0.05 was taken to indicate a significant difference.

Results

The demographic data and patient characteristics were similar in both the groups with a male preponderance and majority patients belonging to 60–70 years age-group (40.7%–46.9%), with only one patient of age less than 50 years in the DLB group (Table 1). On visual analysis, frontal, parietal, temporal and occipital hypometabolism

Fig. 2

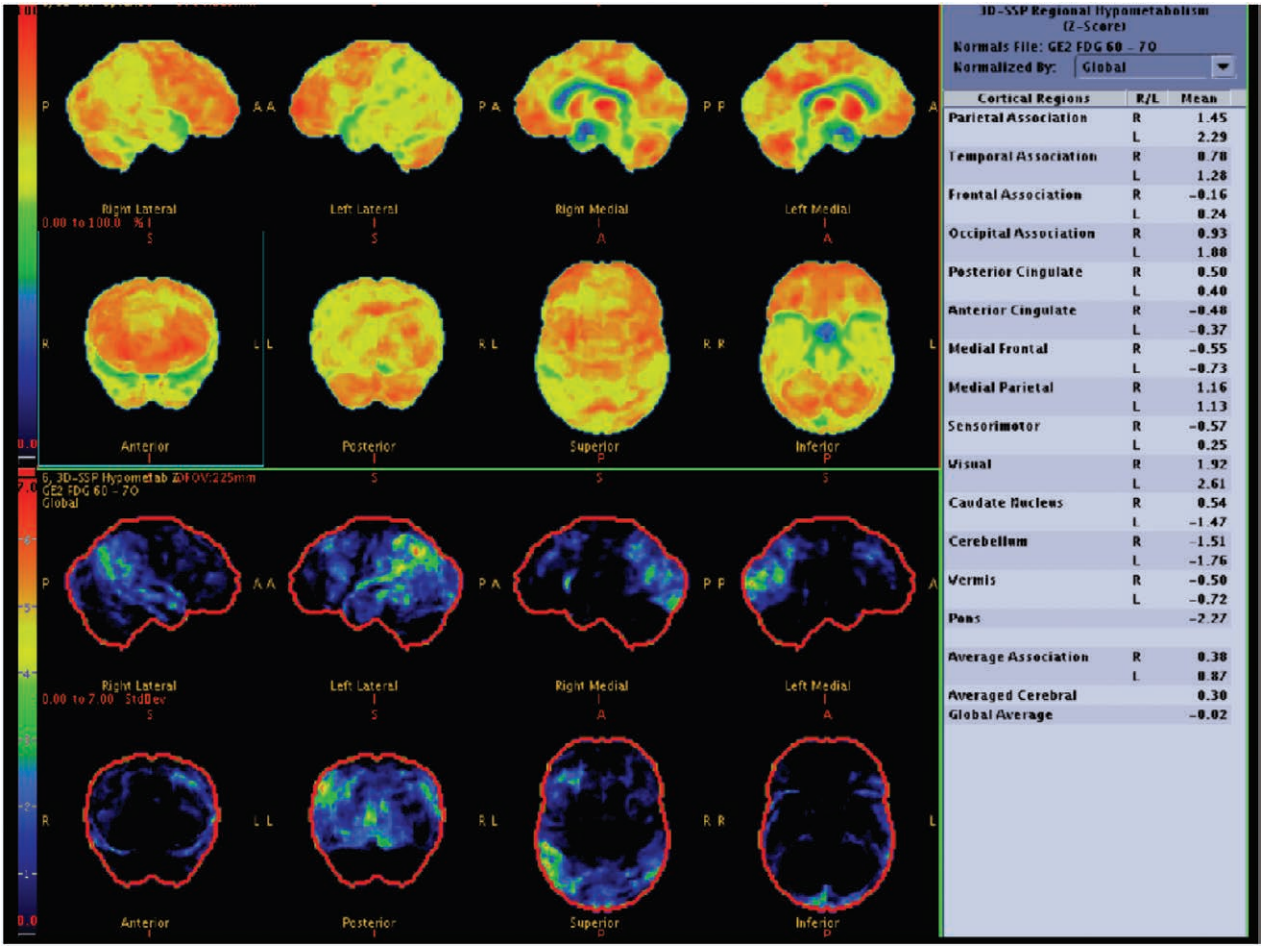

Cortex ID of a 66-year-old male DLB patient showing significant hypometabolism (positive z-score values) in the primary visual cortex, with diffuse hypometabolism in the parieto-temporo-occipital association cortices and posterior cingulate regions. DLB, dementia with Lewy bodies.

was inconstantly found in both the groups; however, sub-cortical and sensori-motor hypometabolism, whenever present, was seen largely in the DLB group.

In the PCA group, lateral occipital cortices were consistently involved. The precuneus and PC cortices were most severely affected. The medial occipital cortex (primary visual cortex) and the sub-cortical structures were relatively spared.

In the DLB group, both medial and lateral occipital cortices demonstrated hypometabolism with variable involvement of the basal ganglia, brainstem and the sensori-motor cortices. The precuneus and PC cortices were affected to a lesser extent, as indicated by the z-score value.

On applying *t*-test to compare the z scores of the hypometabolic regions and test the difference for significance between the two groups, there was significant difference between the z scores of parietal association (PA), temporal association (TA), visual cortex (medial occipital) and PC cortices (Table 2). ROC curve analysis was carried out to determine the significant cut-off values of z scores for each region. The following values were obtained with their respective sensitivity and specificity (Table 3). Binary logistic regression in univariate analysis was applied to these z scores to determine the odds ratio of being in the predicted groups. The cut-off values of three, two and 0.5 had acceptable sensitivity and specificity for PA, TA and PC cortices respectively (Table 4). Binary logistic regression in multivariate analysis was done to determine the odds ratio for being in the DLB group when the z scores are above the cut-off values for each region. The highest odds ratio for being in the DLB group was found in the primary visual cortex with a cut-off z-score of zero (Table 5).

Discussion

As per our review of literature, the present study is the first of its kind to quantitatively incorporate the regional

Table 1 Demographic details and clinical features of patients

Demographic	PCA (n = 34)	DLB (n = 38)	*P* value
Sex (%)			
Male	20 (58.82)	25 (65.79)	0.27
Female	14 (41.18)	13 (34.21)	
Age at onset (years), mean (±SD)	64 (±8.33)	63.8 (±8.87)	0.42
Age at imaging (years), mean (±SD)	66.5 (±8.19)	66.5 (±9.03)	0.48
Disease duration (years), mean (±SD)	2.47(±0.96)	2.69(±1.61)	0.09
MMSE (/30), mean (±SD)	23.53 (±0.96)	23.56 (±1.69)	0.44
Clinical features (%)			
Visuospatial deficits (including synaptapanagnosia, optic ataxia, oculomotor apraxia)	34 (100)	31(81)	0.002
Visual Hallucinations	5 (14.7)	25 (65.79)	<0.00001
REM sleep behaviour disorder	4 (11.76)	26 (68.42)	<0.00001
Parkinsonism	8 (23.53)	36 (94.74)	<0.00001
Fluctuations	0 (0)	37 (97.37)	<0.00001
Autonomic dysfunction	2 (5.82)	10 (26.32)	0.009
Postural imbalance	9	34	<0.00001

DLB, dementia with Lewy bodies; MMSE, mini mental state examination; PCA, posterior cortical atrophy; REM, rapid eye movement.

Table 2 Applying *t*-test to compare the difference in z scores of specific areas between dementia with Lewy bodies and posterior cortical atrophy groups

Regions of hypometabolism	T score	*P* value
Parietal association area (PA)	2.99	0.004[a]
Temporal association area (TA)	−4.3	<0.001[a]
Occipital association area (OA)	1.82	0.07
Visual cortex (V)	5.90	<0.001[a]
Posterior cingulate cortex (PC)	−2.55	0.01[a]
Anterior cingulate cortex (AC)	−1.72	0.09
Sensori-motor cortex (SM)	0.95	0.17

[a]*P* value of <0.05 was considered statistically significant.

Table 3 Receiver operator characteristic analysis to determine the cut-off z scores with their respective sensitivity and specificity to be in either of the predicted groups

Region	Predicted group	Cut off (z score)	Sensitivity (%)	Specificity (%)
PA	PCA	3	65.6	68.7
TA	PCA	2	78	75
PC	PCA	0.5	93.7	40.6
V	DLB	0	87.5	71.9

DLB, dementia with Lewy bodies; PA, parietal association area; PC, posterior cingulate cortex; PCA, posterior cortical atrophy; TA, temporal association area; V, visual cortex.

Table 4 Applying binary logistic regression in univariate analysis to determine the odds ratio of being in respective predicted groups when the z-scores are above the cut-off values for each region

Region (z score > cut-off)	*P* value	Predicted group	Odds ratio	95% confidence interval
PA (>3)	0.01[a]	PCA	3.66	1.30–10.32
TA (>2)	<0.001[a]	PCA	10.71	3.36–34.13
PC (>0.5)	0.01[a]	PCA	7.85	1.57–39.17
V (>0)	<0.001[a]	DLB	24.7	5.99–101.85

DLB, dementia with Lewy bodies; PA, parietal association area; PC, posterior cingulate cortex; PCA, posterior cortical atrophy; TA, temporal association area; V, visual cortex.
[a]*P* value of <0.05 was considered statistically significant.

Table 5 Applying binary logistic regression in multivariate analysis to determine the odds ratio of being in dementia with Lewy bodies group when the z-scores are above the cut-off values for each region

Region (z score > cut-off)	*P* value	Odds ratio	95% confidence interval
PA (>3)	0.19	0.37	0.86–1.66
TA (>2)	0.37	0.49	0.10–2.37
PC (>0.5)	0.14	0.20	0.25–1.69
V (>0)	0.001[a]	15.84	2.90–86.43

PA, parietal association area; PC, posterior cingulate cortex; TA, temporal association area; V, visual cortex.
[a]*P* value of <0.05 was considered statistically significant.

hypometabolism in terms of the z-score values, and also in establishing a predictive model of being in either of the two disease groups using logistic regression analysis by determining the cut-off z scores for each core region of involvement. Our findings are in concordance with previous studies [16,19,20], that showed striking overlap between areas of posterior cortical hypometabolism between the PCA and DLB groups. We have utilized abnormality in [^{99m}Tc]TRODAT SPECT scan to scintigraphically classify patients into the DLB group. This is supported by previous studies done by Walker *et al.* [19,20] utilizing ^{123}I-FP-CIT, which demonstrated decline in the striatal dopaminergic neurons in DLB and PD groups as compared to the AD group [19–25]. There are a miniscule number of reported false negatives DAT scans in DLB patients, which has been explained by the temporal course of DAT imaging. Imaging for DAT was performed early at the onset of symptoms when Parkinsonism was not manifest as regards cognitive and visual symptoms; this was due to later involvement of the nigrostriatal pathway [26–28].

Previous studies done by Whitwell *et al.* [16] comparing PCA and DLB on [^{18}F]FDG PET have utilized the presence of beta-amyloid deposition in the PCA group to confirm the AD pathology. But they could not document the absence of amyloid deposition in the DLB group, as they conducted [^{11}C]PiB amyloid PET in the PCA group only. However, it has been documented that presence of beta-amyloid plaques alone is non-specific for the diagnosis of AD [29] and is a common neuropathological

finding seen in a number of conditions such as vascular dementia [30] and DLB [31,32]. In another study done by Gomperts *et al.* [33], no significant difference was found between the mean amyloid burden in DLB and AD groups, and they reported [^{11}C]PiB retention was significantly higher (*P*-value < 0.05) in the DLB group than in the PD or healthy control groups. To overcome this pitfall, we relied on abnormal DAT based imaging to classify patients in the DLB group, rather than the presence of amyloid deposition for labelling PCA.

Numerous studies have documented the supplementary role of [^{18}F]FDG PET in diagnosing and differentiating PCA from DLB by studying the patterns of hypometabolism in the core regions. We found that although visual analysis revealed significant overlap between the two, quantitative analysis of the z score values (positive z-score indicating hypometabolism relative to normal age-matched controls) yielded better outcomes. We found a statistically significant difference between the mean z scores in the PA, TA, Visual/Medial occipital (V) and PC cortices. Lateral occipital region showed no significant difference between the two groups (*P*-value = 0.07), indicating similar involvement in both PCA and DLB. Mean z scores in the frontal association, anterior cingulate, sensorimotor cortex, and cerebellum were not in the range suggestive of hypometabolism (i.e. had negative z scores) and had no significant difference between PCA and DLB. Hypometabolism (more positive z score) in the PA, TA and PC regions combined together with normal- or hyper-metabolism in the visual cortex was predictive of PCA according to binary logistic regression, both in univariate and multivariate analysis, with their cut-off z scores as given in Table 2. Of these regions, TA region when taken above a cut-off value of two, was found to have the highest odds ratio of 10.71 with an acceptably high sensitivity and specificity (78% and 75%, respectively). The lateral occipital cortex did show hypometabolism in all PCA patients, but due to the overlap with DLB patients, no cut-off score could be established for it. We did not find any region showing greater hypometabolism in PCA group than that in DLB group. This is shown in Fig. 3, where areas of significant overlap (in blue) and differences (in red) between the DLB and PCA groups on voxel-level maps of SPM analysis. The areas of differences being those, that showed hypometabolism in DLB group over PCA group. This invariably suggests that all these areas had varying degrees of hypometabolism in the DLB group as well. Univariate logistic regression suggested that the hypometabolism in the visual cortex alone had a highly significant Odds ratio of 24.7 to predict classification of patients in DLB group (*P*-value <0.001). This was further validated by applying multivariate analysis considering all four core regions (PA, TA, PC, V) with z scores above their cut-off values, to develop a prediction model for DLB, which demonstrated only visual cortex to have significant odds ratio with *P*-value <0.001.

Fig. 3

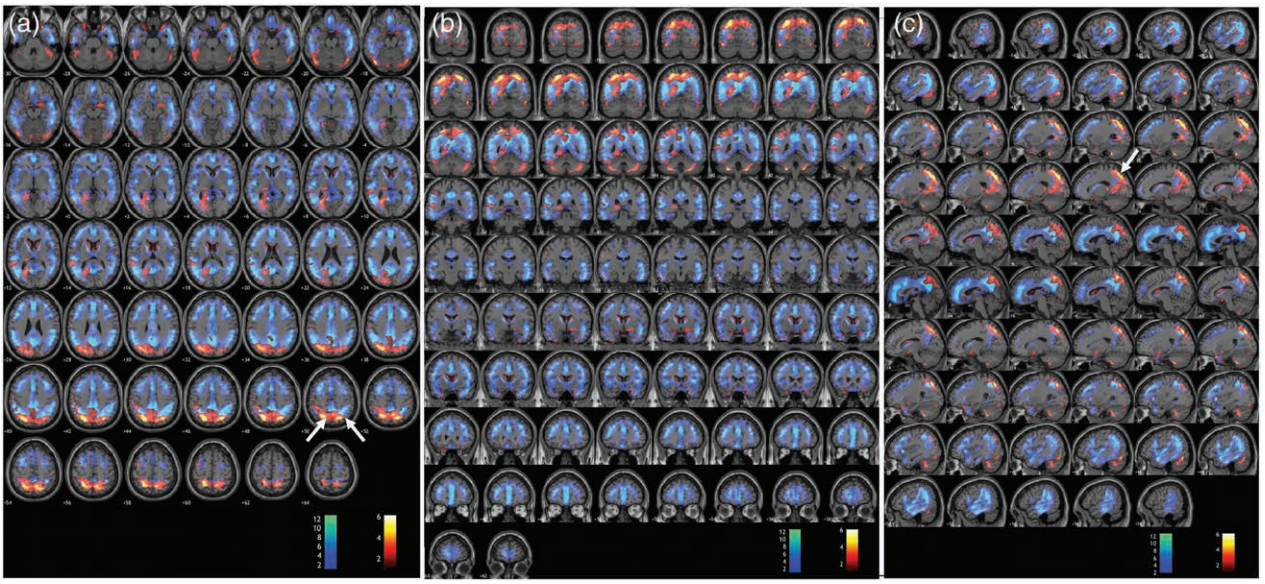

Fused FDG-PET/MRI images in (a) axial, (b) coronal and (c) sagital sections showing regions of overlap (blue) between PCA and DLB using conjunction analysis and regions that showed greater hypometabolism in DLB than PCA on direct comparison (red). Results are shown after correction for multiple comparisons at *P*-value <0.05. Arrows show areas of significant hypometabolism in the DLB group as compared to the PCA group. DLB, dementia with Lewy bodies; PCA, posterior cortical atrophy.

Significant difference existed between the z scores of PC cortex of the two groups, with higher z scores (more than cut-off value of 0.5), being more predictive of PCA (odds ratio = 7.85, sensitivity = 93.7%). However, PC cortex showed variable hypometabolism in the DLB patients who had predominant cognitive impairment, and absence of PC involvement was noted in few PCA patients who had predominant visuospatial deficits [12,25]. This finding is in agreement with the previous studies that demonstrated poor specificity of the 'cingulate island sign' in ruling out PCA (specificity in our study = 40.6%).

A limitation of our study was that partial volume correction could not be applied during SPM and z score analysis. Also, we did not find any significant asymmetry in our PCA patients, as has been mentioned in previous studies that demonstrated more hypometabolism on the right side [16,34].

Conclusion

Our findings support the evidence in recognizing signature patterns of hypometabolism on [^{18}F]FDG PET in patients suspected of having PCA or DLB. Primary visual cortex hypometabolism can serve as an independent diagnostic marker for DLB, even in the absence of supportive DAT imaging and warrants further prospective studies with follow-up data. This study provides valuable insight into the phenotypical and imaging overlaps between PCA and DLB, and can thus help in better utilization of [^{18}F]FDG PET in such ambiguous clinical settings.

Acknowledgements

Data selected for SNMMI 2019 poster presentation and published as abstract: Vanshika Gupta, Ritu Verma, Rajeev Ranjan, Ethel Belho, Harsh Mahajan. Lewy body dementia and posterior cortical variant of Alzheimer's disease: distinguishing imaging patterns based on 18F-FDG PET/CT and 99mTc-TRODAT SPECT scan. *J Nucl Med* 2019; 60 (1):1491.

Conflicts of interest

There are no conflicts of interest.

References

1 Benson DF, Davis RJ, Snyder BD. Posterior cortical atrophy. *Arch Neurol* 1988; **45**:789–793.
2 Tang-Wai DF, Graff-Radford NR, Boeve BF, Dickson DW, Parisi JE, Crook R, *et al*. Clinical, genetic, and neuropathologic characteristics of posterior cortical atrophy. *Neurology* 2004; **63**:1168–1174.
3 McKeith IG, Dickson DW, Lowe J, Emre M, O'Brien JT, Feldman H, *et al*.; Consortium on DLB. Diagnosis and management of dementia with Lewy bodies: third report of the DLB consortium. *Neurology* 2005; **65**:1863–1872.
4 McKeith I, O'Brien J, Walker Z, Tatsch K, Booij J, Darcourt J, *et al*.; DLB Study Group. Sensitivity and specificity of dopamine transporter imaging with 123I-FP-CIT SPECT in dementia with Lewy bodies: a phase III, multicentre study. *Lancet Neurol* 2007; **6**:305–313.
5 Minoshima S, Foster NL, Sima AA, Frey KA, Albin RL, Kuhl DE. Alzheimer's disease versus dementia with Lewy bodies: cerebral metabolic distinction with autopsy confirmation. *Ann Neurol* 2001; **50**:358–365.
6 Albin RL, Minoshima S, D'Amato CJ, Frey KA, Kuhl DA, Sima AA. Fluoro-deoxyglucose positron emission tomography in diffuse Lewy body disease. *Neurology* 1996; **47**:462–466.
7 Gilman S, Koeppe RA, Little R, An H, Junck L, Giordani B, *et al*. Differentiation of Alzheimer's disease from dementia with Lewy bodies utilizing positron emission tomography with [18F]fluorodeoxyglucose and neuropsychological testing. *Exp Neurol* 2005; **191** (Suppl 1):S95–S103.
8 Ishii K, Imamura T, Sasaki M, Yamaji S, Sakamoto S, Kitagaki H, *et al*. Regional cerebral glucose metabolism in dementia with Lewy bodies and Alzheimer's disease. *Neurology* 1998; **51**:125–130.
9 Nestor PJ, Caine D, Fryer TD, Clarke J, Hodges JR. The topography of metabolic deficits in posterior cortical atrophy (the visual variant of Alzheimer's disease) with FDG-PET. *J Neurol Neurosurg Psychiatry* 2003; **74**:1521–1529.
10 Rosenbloom MH, Alkalay A, Agarwal N, Baker SL, O'Neil JP, Janabi M, *et al*. Distinct clinical and metabolic deficits in PCA and AD are not related to amyloid distribution. *Neurology* 2011; **76**:1789–1796.
11 Wang XD, Lu H, Shi Z, Cai L, Liu S, Liu S, *et al*. A pilot study on clinical and neuroimaging characteristics of Chinese posterior cortical atrophy: comparison with typical Alzheimer's disease. *Plos One* 2015; **10**:e0134956.
12 Graff-Radford J, Murray ME, Lowe VJ, Boeve BF, Ferman TJ, Przybelski SA, *et al*. Dementia with Lewy bodies: basis of cingulate island sign. *Neurology* 2014; **83**:801–809.
13 Imamura T, Ishii K, Sasaki M, Kitagaki H, Yamaji S, Hirono N, *et al*. Regional cerebral glucose metabolism in dementia with Lewy bodies and Alzheimer's disease: a comparative study using positron emission tomography. *Neurosci Lett*. 1997; **235**:49–52.
14 Lim SM, Katsifis A, Villemagne VL, Best R, Jones G, Saling M, *et al*. The 18F-FDG PET cingulate island sign and comparison to 123I-beta-CIT SPECT for diagnosis of dementia with Lewy bodies. *J Nucl Med* 2009; **50**:1638–1645.
15 Singh TD, Josephs KA, Machulda MM, Drubach DA, Apostolova LG, Lowe VJ, Whitwell JL. Clinical, FDG and amyloid PET imaging in posterior cortical atrophy. *J Neurol* 2015;**262**:1483–1492.
16 Whitwell JL, Graff-Radford J, Singh TD, Drubach DA, Senjem ML, Spychalla AJ, *et al*. 18F-FDG PET in posterior cortical atrophy and dementia with Lewy bodies. *J Nucl Med* 2017; **58**:632–638.
17 Sateia MJ, Reed VA, Christian Jernstedt G. The Dartmouth sleep knowledge and attitude survey: development and validation. *Sleep Med* 2005; **6**:47–54.
18 Ashburner J, Friston KJ. Voxel-based morphometry–the methods. *Neuroimage* 2000; **11**:805–821.
19 Walker Z, Costa DC, Walker RW, Shaw K, Gacinovic S, Stevens T, *et al*. Differentiation of dementia with Lewy bodies from Alzheimer's disease using a dopaminergic presynaptic ligand. *J Neurol Neurosurg Psychiatry* 2002; **73**:134–140.
20 Walker Z, Jaros E, Walker RW, Lee L, Costa DC, Livingston G, *et al*. Dementia with Lewy bodies: a comparison of clinical diagnosis, FP-CIT single photon emission computed tomography imaging and autopsy. *J Neurol Neurosurg Psychiatry* 2007; **78**:1176–1181.
21 Donnemiller E, Heilmann J, Wenning GK, Berger W, Decristoforo C, Moncayo R, *et al*. Brain perfusion scintigraphy with 99mtc-HMPAO or 99mtc-ECD and 123I-beta-CIT single-photon emission tomography in dementia of the Alzheimer-type and diffuse Lewy body disease. *Eur J Nucl Med* 1997; **24**:320–325.
22 Hu XS, Okamura N, Arai H, Higuchi M, Matsui T, Tashiro M, *et al*. 18F-fluorodopa PET study of striatal dopamine uptake in the diagnosis of dementia with Lewy bodies. *Neurology* 2000; **55**:1575–1577.
23 Ito K, Nagano-Saito A, Kato T, Arahata Y, Nakamura A, Kawasumi Y, *et al*. Striatal and extrastriatal dysfunction in Parkinson's disease with dementia: a 6-[18F]fluoro-L-dopa PET study. *Brain* 2002; **125**:1358–1365.
24 Koeppe RA, Gilman S, Junck L, Wernette K, Frey KA. Differentiating Alzheimer's disease from dementia with Lewy bodies and Parkinson's disease with (+)-[11C]dihydrotetrabenazine positron emission tomography. *Alzheimers Dement* 2008; **4**:S67–S76.
25 O'Brien JT, Colloby SJ, Fenwick J, Williams ED, Firbank M, Burn D, *et al*. Dopamine transporter loss visualized with FP-CIT SPECT in the differential diagnosis of dementia with Lewy bodies. *Arch Neurol* 2004; **61**: 919–925.
26 Thomas AJ, Attems J, Colloby SJ, O'Brien JT, McKeith I, Walker R, *et al*. Autopsy validation of 123I-FP-CIT dopaminergic neuroimaging for the diagnosis of DLB. *Neurology* 2017; **88**:276–283.
27 van der Zande JJ, Booij J, Scheltens P, Raijmakers PG, Lemstra AW. [(123)] FP-CIT SPECT scans initially rated as normal became abnormal over time in patients with probable dementia with Lewy bodies. *Eur J Nucl Med Mol Imaging* 2016; **43**:1060–1066.

28 Nobili F, Arnaldi D, Morbelli S. Is dopamine transporter invariably impaired at the time of diagnosis in dementia with Lewy bodies? *Eur J Nucl Med Mol Imaging* 2016; **43**:1056–1059.
29 Perl DP. Neuropathology of Alzheimer's disease. *Mt Sinai J Med* 2010; **77**:32–42.
30 Alonzo NC, Hyman BT, Rebeck GW, Greenberg SM. Progression of cerebral amyloid angiopathy: accumulation of amyloid-beta40 in affected vessels. *J Neuropathol Exp Neurol* 1998; **57**:353–359.
31 Ballard C, Ziabreva I, Perry R, Larsen JP, O'Brien J, McKeith I, *et al*. Differences in neuropathologic characteristics across the Lewy body dementia spectrum. *Neurology* 2006; **67**:1931–1934.
32 Tsuboi Y, Dickson DW. Dementia with Lewy bodies and Parkinson's disease with dementia: are they different? *Parkinsonism Relat Disord* 2005; **11** (Suppl 1):S47–S51.
33 Gomperts SN, Rentz DM, Moran E, Becker JA, Locascio JJ, Klunk WE, *et al*. Imaging amyloid deposition in Lewy body diseases. *Neurology* 2008; **71**:903–910.
34 Spehl TS, Hellwig S, Amtage F, Weiller C, Bormann T, Weber WA, *et al*. Syndrome-specific patterns of regional cerebral glucose metabolism in posterior cortical atrophy in comparison to dementia with Lewy bodies and Alzheimer's disease–a [F-18]-FDG pet study. *J Neuroimaging* 2015; **25**:281–288.